INVESTIGATION OF THE EFFECT OF DEPOSIT LAYER ON HEAT TRANSFER IN THE TRIGA MARK-II NUCLEAR RESEARCH REACTOR COOLING SYSTEM

by

Orhan Erdal AKAY [a*] ***and Mehmet DAS*** [b]

[a] Faculty of Engineering and Architecture, Mechanical Engineering Department, Kahramanmaras Sutcuimam University, Kahramanmaras, Turkey
[b] Mechatronics Engineering Department, Engineering Faculty, Fırat University, Elazig, Turkey

Original scientific paper
https://doi.org/10.2298/TSCI220116065A

In this presented study, the cooling problem of the I.T.U. Triga Mark-II reactor has been handled and analyzed, and solutions were proposed. First of all, a thermal model of the reactor, heat exchanger, and cooling tower trio was established in the reactor. With this model, which was obtained with the help of experimental data, the parameters affecting the change of reactor water temperature over time were determined, and significant findings were obtained by investigating the possibilities of increasing the cooling power of the existing system. Then, using these mathematical equations, the effects of parameters that can affect the power of the reactor cooling system are investigated. The parameters affecting the cooling power are the cooling water flow rates in the second cooling circuits and the deposited layer that may exist as a result of numerical calculations. Different models have been created with machine learning algorithms (page regression, decision tree) to estimate the effect of the deposit layer. The mathematical and predictive models obtained with the experimental data for the heat transfer coefficient of the deposit layer, h_{bd}, were compared. The pace regression algorithm modeled the h_{bd} values with the least error rate (RMSE: 1.66) among the models. It has been calculated that the average tank water temperature will decrease by approximately 3.5 °C if the deposits layer is cleared.

Key words: *Triga Mark-II, heat exchanger, deposit layer, equation derivation, heat transfer coefficient, machine learning algorithm*

Introduction

Due to the properties of the fluid used in the heat exchangers, a deposits layer (*i.e.*, lime, particles, residue) occurs on the heat exchanger surface over time. As a result of this situation, the thermal efficiency of the heat exchanger decreases, and accordingly, the fuel consumption increases. Many studies on different subjects related to the deposit layer formed in the heat exchangers are given in tab. 1. In these studies, the system in which the depositional layer was examined and its effects were taken into account. The adverse effects of the deposition layer, which is a negative factor for heat exchangers, have been studied in detail.

Built for education and research purposes, the upper limit given for the average tank water temperature of the Triga Mark-II reactor is 43.1 °C [1, 2]. However, due to the insufficient

* Corresponding authors, e-mails: akayorhan@ksu.edu.tr, mehmet.das@gop.edu.tr

Tabel 1. Experimental studies related to the deposit layer in the literature

The part in which the deposit layer was examined	Researched attribute	The effect of deposits	Ref.
Tubes from the super heater of a lignite utility boiler	Heat transfer rate	A reduction of 8-17% in the heat transfer rate because of deposition	[3]
Compact heat exchanger	Effects of deposit particle size in the range of 1 μm to 4 mm on the pressure drop in the heat exchanger	Particle deposit increased the pressure drop of the heat exchanger	[4]
The tube bundle heat exchanger	Efect of flue gas velocity on relative deposition ratio	At the same fluid velocity, the relative deposition rate of particles with a diameter of 5 μm is greatest and that of particles with a diameter of 10 μm is the smallest	[5]
Pressurized water reactor	Corrosion-related unidentified deposit (CRUD)	Radial CRUD deposit layer is highest in the flow range between 7 m/s and 15 m/s. The deposit carried by the fluid and formed into the particles increased the electrokinetic effects occurring at high speeds	[6]
Shell and tube heat exchanger in petroleum refineries	Asphaltenes deposition	It was determined with the help of CFD simulation that the deposit layer of asphalt particles in the heat exchanger occurred in the back cover of the heat exchanger and in the lower pipe layer	[7]
Rectangular heat exchanger channel	The deposition of gas-side fly ash particles on the heating surface	The ceiling and side walls of the heat exchanger have less deposition efficiency than the floor part	[8]
The helium flow in intermediate heat exchanger	Graphite particle deposition on the deflector at the entrance passage of the intermediate heat exchanger	The particle deposition rate at the deflector inlet of the intermediate heat exchanger decreases first and then increases in the inlet path of the intermediate heat exchanger	[9]
Surface of boilers	Ash particles deposition	Serbian coal slag values (lignitic-type-ash coals) showed a tendency to form deposits in boiler heating	[10]
Plate-fin heat exchangers	Effect of deposits on fluid inlet velocity and temperature difference in plate heat exchangers	As the critical air velocity in the heat exchanger increases, the particle deposition rate decreases, and as the particle size increases, the deposition increases. The temperature difference increased the average deposition efficiency of 1μm particles and decreased the average deposition efficiency of 7 μm particles	[11]
Plate heat exchangers	Effect of deposit on heat exchanger inlet and outlet on themal efficiency	The deposit reduces the efficiency of the heat exchangers and makes the cleaning process increasingly difficult	[12]
The circular tube bundle heat exchanger	Investigation of the effects of longitudinal pipe spacing, transverse pipe spacing and pipe geometry on deposit formation	Elliptical tube bundles reduced deposit formation	[13]

cooling system, the average tank water temperature at high powers rises above this given temperature limit, especially in summer [14]. The tendency of the temperature to exceed the given upper limit values increases the humidity rate on and around the pool surface. For this reason, the risk of corrosion and failure in mechanical, electrical, and electronic systems increases, and the risk of corrosion increases in materials in contact with cooling water [1, 2]. In addition, the resin of demineralizer in the tank water treatment system loses its properties rapidly due to high temperature and can eventually deteriorate completely [2].

In this presented study, the cooling problem of the nuclear reactor was analyzed within the scope of the problems mentioned in the previous paragraph. For this, first of all, in the Triga Mark-II reactor, the reactor-heat exchanger thermal model has been established [15]. With the help of this model and experimental data, variation of the reactor tank water temperature was determined. In order to construct the thermal model of the nuclear reactor cooling system, it has been assumed that the reactor operates at a specific constant power. Tank water temperature values were measured from seven different points [16]. Mathematical equations that give the time-dependent variation of the cooling water, temperature values, and total heat transfer values in the reactor tank and heat exchanger, respectively, were solved with the Wolfram Mathematica software non-Linear fit model [15]. Then, using this mathematical model, the parameters that could affect the power of the reactor's cooling system were investigated. The extent to which changing the flow rates and clearing the deposit layer can improve the cooling power has been investigated. In addition, the deposit layer effect affecting the total heat transfer coefficient of the reactor cooling system and the reactor tank water temperature was estimated by the decision tree algorithm, a machine learning algorithm. The results of the predictive model obtained and the mathematical model obtained with the experimental data have been obtained pretty similar to each other.

Material and methods

Triga Mark-II nuclear research reactor cooling system

The cooling system of the Triga Mark-II reactor examined in this study consists of two parts, fig. 1. These are a tube-enveloped cross-flow heat exchanger, and a cooling tower connected to the tube-enveloped cross-flow heat exchanger [1]. The geometric dimensions and manufacturing features of the heat exchanger u were taken from the study of Akay and Das [15].

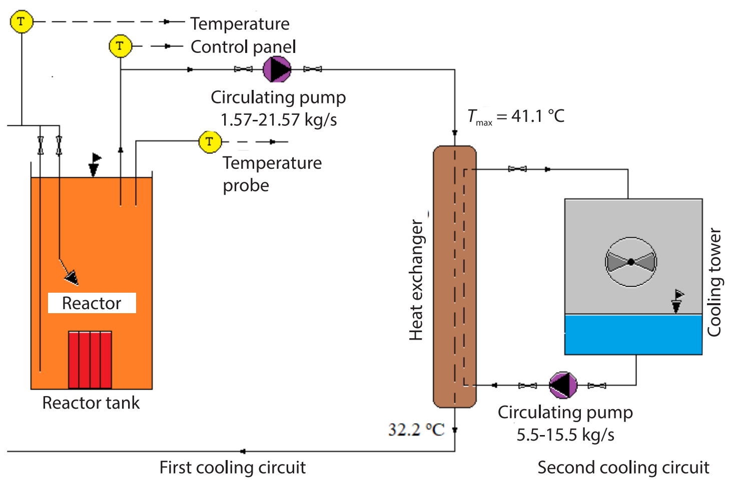

Figure 1. First and second cooling circuit diagram of Triga Mark-II nuclear research reactor [17]

In the first cooling circuit, the reactor core is cooled as follows. The thermal energy produced in the fuel elements in the reactor core is drawn through the natural-convection of water in the tank. The heated water rises towards the tank surface and is sent to the heat exchanger by being absorbed by the first circuit circulation pump 90 cm below the surface. By transferring the thermal energy drawn from the reactor core through the heat exchanger to the water circulating in the second cooling circuit, the cooled water returns to the reactor core to continue its cooling function. The heat exchanger working principal diagram is given in fig. 2. The heat exchanger is manufactured with a total of seven passes. Six of these passages are on the side of the first circuit of the cooling section, and one passage is on the side of the second circuit. Tube bundles in the heat exchanger connect both circuits with the body of the heat exchanger.

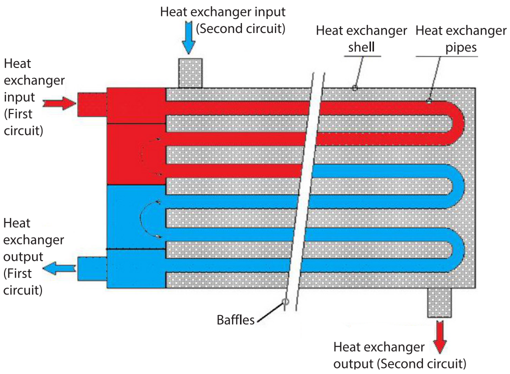

Figure 2. Shell and tube heat exchanger working principle

In fig. 2, the flow flowing from the inside of the heat exchanger (inside the pipe) is used in the first circuit of the cooling system, and the flow from the outside (shell) is used in the second circuit.

This study investigated the effects of the deposit layer that the fluid can form in the pipe interior on heat transfer. The effects of deposits that may occur at different fluid-flow rates in the pipe have been investigated. In fig. 3, the representation of the deposits layer that is likely to form in the pipe is given. The mass-flow rate change of the fluid has been selected according to the allowable operating temperature range of the reactor [1].

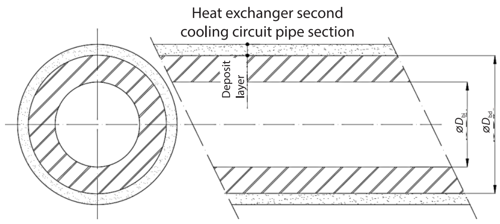

Figure 3. Deposit layer in pipe

The reactor heat exchanger design features used in the calculations are given in tab. 2. In this table, detailed specifications of one of the reactor and the second cooling circuits are given.

Table 2. Basic design features and geometric dimensions of the reactor heat exchanger [1, 2]

Design features	First cooling circuit	Second cooling circuit
Mass-flow rate	1.57-21.57 kg/s	5.5-15.5 kg/s
Inlet temperature	41.1 °C	26.7 °C
Outlet temperature	32.2 °C	32.2 °C
Operation pressure	7.95 · 105 Pa	$7.95 \cdot 10^5$ Pa
Design temperature	150 °C	150 °C
Material	SS-304 stainless steel	Non-alloy steel
Total area	24.84 m^2 (inner surface)	31.78 m^2 (outer surface)
Inner diameter	$2.09 \cdot 10^{-2}$ m (pipe)	$3.56 \cdot 10^{-1}$ m (Shell)
Outer diameter	$2.67 \cdot 10^{-2}$ m (pipe)	_
Number of fluid passes	6	1
Number	112 pipes	1 shell
Flow cross-sectional area	$6.51 \cdot 10^{-3}$ m^2	$6.09 \cdot 10^{-2}$ m^2

The flow chart expressing the research process headings of this presented computational study is given in fig. 4.

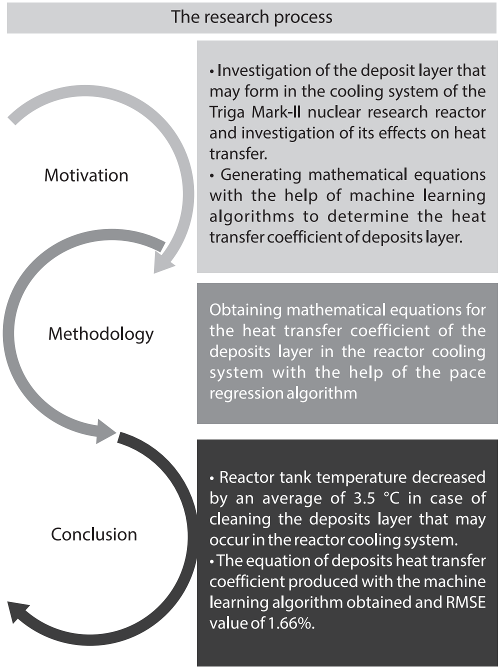

Figure 4. The flow chart expressing the process of this work

Determination of the heat transfer coefficients of the reactor cooling system

In the heat transfer coefficient calculations of the shell-tube-envelope heat exchangers, it is complicated to calculate the heat transfer coefficient of the heat exchanger because the flow inside the envelope is irregular and complex. The heat transfer values found in this type of heat exchanger theory cannot be expected to be very close to the actual values. The immeasurable dimensions of the envelope curtains in the heat exchanger and the complexity of the fluid regime increase error of calculation heat transfer of the heat exchanger [17]. In addition this, the deposit has probably formed on the outer surface of the pipes of the heat exchanger since no maintenance has been done to the interior for a long time and the water lost in the circuit is supplied directly from the city network as a result of the malfunctioning of the softener units. This situation is another factor that can increase the uncertainty of the result to be obtained with theoretical calculations.

For the aforementioned reasons, the heat exchangers' total heat transfer coefficient values should be calculated based on experimental data. In this study, temperature data taken from seven different points was used when the reactor in the experimental study for the Traiga Mark-II nuclear research reactor was operating with 200 kW power [17]. Equation (1) expression is fitted to these data using the least-squares method (adapted) [16]. As a result of this fit process, the tank water weight coefficient and the total heat transfer coefficient and its components, the heat transfer coefficients, and the heat transfer coefficient of a possible deposit, were found. In order for the fit process to converge more healthily and faster, the convection coefficients, which can be calculated in order, were calculated theoretically and used as the initial value data:

$$T_R(t) = (1-a)\left[T_{Kc} + \frac{(1-\varepsilon)P_R}{\dot{m}_1 c_P \varepsilon}\left(1-\exp\left\{\frac{\dot{m}_1 c_P \varepsilon}{c_p\left[1-\varepsilon(1-a)\right]}(t_1 - t)\right\}\right)\right] +$$
$$+a\left[T_{Kc} + \frac{P_R}{\dot{m}_1 c_P \varepsilon}\left(1-\exp\left\{\frac{\dot{m}_1 c_P \varepsilon}{c_p\left[1-\varepsilon(1-a)\right]}(t_1 - t)\right\}\right)\right] \tag{1}$$

Equation (1) is derived from eqs. (2) and (3), which expresses the variation of reactor inlet and outlet temperatures over time in Akay and Das's work [15]. Akay determined the inlet temperature of the reactor according to the energy balance between the cooling system and the reactor. Then he expressed the second circuit inlet temperature of the cooling system with eq. (4) [2]:

$$T_{Ri}(t) = T_{Kc} + \frac{(1-\varepsilon)P_R}{\dot{m}_1 c_p \varepsilon}\left[1-\exp\left(\left\{\frac{\dot{m}_1 c_p \varepsilon}{c_p\left[1-\varepsilon(1-a)\right]}\right\}(t_1 - t)\right)\right] \tag{2}$$

$$T_{Ro}(t) = T_{Kc} + \frac{P_R}{\dot{m}_1 c_p \varepsilon}\left[1-\exp\left(\left\{\frac{\dot{m}_1 c_p \varepsilon}{c_p\left[1-\varepsilon(1-a)\right]}\right\}(t_1 - t)\right)\right] \tag{3}$$

$$\dot{m}_1 c_p\left[T_{Ro}(t) - T_{Ri}(t)\right] = \dot{m}_2 c_p\left[T_{Kc}(t) - T_{Kg}(t)\right] \tag{4}$$

If eqs. (2) and (3) are arranged according to eqs. (4) and (5), which gives the cooling tower inlet temperature variation with time, is obtained. Thus, the average temperature of the reactor tank water can be calculated with eq. (1), and the cooling tower inlet water temperature can be calculated:

$$T_{Kg}(t) = \frac{\dot{m}_1}{\dot{m}_2}\left[\left[T_{Kc} + \frac{P_R}{\dot{m}_1 c_p \varepsilon}\left[1-\mathrm{e}^{\left[\frac{\dot{m}_1 c_p \varepsilon}{c_p\left[1-\varepsilon(1-a)\right]}\right](t_1 - t)}\right]\right] - \right.$$
$$\left. - \left[T_{Kc} + \frac{(1-\varepsilon)P_R}{\dot{m}_1 c_p \varepsilon}\left[1-\mathrm{e}^{\left[\frac{\dot{m}_1 c_p \varepsilon}{c_p\left[1-\varepsilon(1-a)\right]}\right](t_1 - t)}\right]\right]\right] + T_{Kc} \tag{5}$$

Determination of deposit effect in reactor cooling system

The heat transfer coefficient of the second circuit side, the heat transfer coefficient of the deposit on the pipes of the heat exchanger, and the average tank water temperature weight coefficient, a, which relates the average tank water temperature with the inlet and outlet temperatures, have been determined with the help of curve fitting to the experimental data. The expression be subjected to curve fitting is eq. (1), which gives the average tank water temperature variation over time. Equation (1) depends on the parameter, ε, and the weight coefficient, a. The ε parameter has been expressed in eq. (7) [18] in terms of NTU and R in eq. (6) expression [19]:

$$NTU = \frac{1}{\sqrt{1+R^2}}\ln\left[\frac{2-(1+R-\sqrt{1+R^2})\varepsilon}{2-(1+R+\sqrt{1+R^2})\varepsilon}\right] \tag{6}$$

$$\varepsilon = \left[\frac{2\left[1-\mathrm{e}^{NTU\sqrt{1+R^2}}\right]}{1+R-\sqrt{1+R^2}-(1+R+\sqrt{1+R^2})\mathrm{e}^{NTU\sqrt{1+R^2}}}\right] \tag{7}$$

The R parameter is found by dividing the first circuit mass-flow value by the second circuit mass-flow value. However, in order to know the NTU, it is necessary to know the total heat transfer coefficient, U, of the heat exchanger. The U depends on knowing the heat transfer coefficients on the first-second circuit side of the heat exchanger and the heat transfer coefficient of the possible deposit layer. Since the flow geometry is smooth on the first circuit side and it is a type of flow where many healthy correlations can be found, eqs. (10)-(18), which were calculated theoretically and depended on, were used for the convection coefficient of this side [20]. Equations (8) and (9) [21] were used to determine the flow characteristics values of the first and second cooling cycles. Equation (7) was used to calculate Reynolds number values, and eq. (8) was used to calculate flow velocity values. The parameters obtained by eqs. (8) and (9) were used in eqs. (10)-(13):

$$\mathrm{Re} = \frac{VD}{\nu} \tag{8}$$

$$V = \frac{\dot{m}}{\rho_s A_k} \tag{9}$$

$$\mathrm{Nu} = 0.023\,\mathrm{Re}^{0.8}\,\mathrm{Pr}^{n} \tag{10}$$

$$\mathrm{Nu} = \frac{hD_h}{\lambda_s} \tag{11}$$

In eq. (8), the value of ν is 0.3. According to the average tank water temperature (TR) value (36.5 °C), λ_s value is 0.622 W/m°C, D_{bi} value for the first cooling circuit is $2.9 \cdot 10^{-2}$ and Prandtl number value is 4.728. Equations (12) and (13) are obtained when the Reynolds number is written as a function of $\dot{m}_1$ according to these values:

$$\mathrm{Re} = \frac{34243}{7.57}\dot{m}_1 = 4.52 \cdot 10^3\,\dot{m}_1 \tag{12}$$

$$\mathrm{Nu} = 35.95\dot{m}_1^{0.8} \tag{13}$$

Using eq. (13) and (11) [22], the heat transfer coefficient of the first circuit side of the heat exchanger, h_1, is expressed by eq. (14) according to the $\dot{m}_1$ value:

$$h_1 = \frac{\dot{m}_1^{0.8}}{9.35 \cdot 10^{-4}} \tag{14}$$

In order to determine the heat transfer coefficient, h_2, of the second cooling circuit side of the heat exchanger, the same procedure was followed for the first circuit. Average values of reactor second cooling circuit water design temperatures are used for kinematic viscosity and Prandtl number. Calculations were made by taking the kinematic viscosity, ν, value of $0.801 \cdot 10^{-6}$ m^2/s and the Prandtl number value of 5.43 according to the average water temperature of 29.45 °C for the second cooling circuit [17]. The shell of the second circuit of the heat exchanger are made of non-alloy steel, and the D_{bd} value is $1.39 \cdot 10^{-2}$ m. In addition, the thermal conductivity coefficient, λ_w, is 16.3 W/m°C for the same average water temperature of 29.45 °C [17].

The Reynolds number can be calculated according to the number $\dot{m}_2$:

$$\mathrm{Re} = \frac{5258}{11.11}\dot{m}_2 = 4.7 \cdot 10^2\,\dot{m}_2 \tag{15}$$

The heat transfer coefficient, h_2, of the second circuit of the heat exchanger was calculated with eq. (17) obtained by using eqs. (10) and (11):

$$\frac{h_2 1.39 \cdot 10^{-2}}{0.622} = 0.023 \cdot 137.30\dot{m}_2^{0.8}\,5.43^{0.3} \tag{16}$$

$$h_2 = \frac{\dot{m}_2^{0.8}}{4.27 \cdot 10^{-3}} \tag{17}$$

The total heat transfer coefficient, U, which is defined according to the second circuit surface area in the heat exchangers, is expressed:

$$U = \frac{1}{\dfrac{1}{h_2} + \dfrac{1}{h_{bd}} + \dfrac{(D_{bd} - D_{bi})}{2\lambda_w}\dfrac{D_{bd}}{D_{lm}} + \dfrac{D_{bd}}{h_{bi}D_{bi}} + \dfrac{D_{bd}}{h_1 D_{bi}}} \tag{18}$$

where h_{bi} and h_{bd} are the heat convection coefficients of the deposits that may occur in the pipe's inner (first circuit) and outer (secondary circuit) parts, respectively, D_{lm} – the logarithmic average of the pipe inner and outer diameters. Equation (19) was used in D_{lm} calculations [23]:

$$D_{lm} = \frac{D_{bd} - D_{bi}}{\ln \dfrac{D_{bd}}{D_{bi}}} \tag{19}$$

Since high purity water is used in the first circuit, it is assumed that there is no lime layer or deposit on the inner surfaces of the heat exchanger pipe. For this reason, it is expected that the deposit layer can only form on the outer surfaces of the tubes (shell) that come into contact with the second circuit water. Thus, the second circuit convection coefficient, the heat convection coefficient of the deposit, and the weight coefficient, a, were chosen as unknowns. As a result, the total heat transfer coefficient during the fit process has been expressed by eq. (20) using eqs. (14), (17), and (18):

$$U = \frac{1}{\dfrac{1}{h_{bd}} + \dfrac{4.27 \cdot 10^{-3}}{\dot{m}_2^{0.8}} + \dfrac{0.0267}{2 \cdot 16.3}\ln\left(\dfrac{0.0267}{0.0209}\right) + \dfrac{0.0267}{0.0209}\dfrac{9.35 \cdot 10^{-4}}{\dot{m}_1^{0.8}}} \tag{20}$$

Equation (21) is obtained as a result of editing the expression eq. (20):

$$U = \frac{1}{\dfrac{1}{h_{bd}} + \dfrac{0.00427}{m_2^{0.8}} + 2.0059 \cdot 10^{-4} + \dfrac{0.0011937}{\dot{m}_1^{0.8}}} \tag{21}$$

Equation (22) has been obtained using values of 0.0011937 for the coefficient c_1 and 0.00427 for the coefficient c_2 and replacing $1/h_{bd}$ with d:

$$U = \frac{1}{d + \dfrac{c_2}{\dot{m}_2^{0.8}} + 2.0059 \cdot 10^{-4} + \dfrac{c_1}{\dot{m}_1^{0.8}}} \tag{22}$$

In eq. (22), parameter d expresses the heat transfer coefficient of the deposit layer under reactor operating conditions. Different c_1 and c_2 values were obtained for each flow rate and heat transfer coefficient values were obtained by using these constant values.

Machine learning algorithm

Machine learning is described as a paradigm of methods that makes various inferences from existing data using statistical and mathematical methods and makes predictions on the unknown with these inferences [24, 25]. They are computer algorithms that model a given problem according to the data obtained from the environment of the problem [26, 27]. In the present study, decision tree regression (M5P) and pace regression algorithms are used to model deposit heat transfer coefficient values. The input and output parameters used for the structure of the models in machine learning algorithms are given in tab. 3.

A total of 425 data were used in the modelling of the heat transfer coefficient of the deposit, which causes negative effects in the cooling system. The 125 data were used to test the model to be created in this data set, and 300 data were used to train it. Ten-Cross validation method was used for data validation. Cross-validation was a technique used in model selection better predict the error of a test in a machine learning model [28, 29]. The regression Learner tab in MATLAB 2018b software was used to model h_{bd} data.

Table 3. Parameters in the dataset used for machine learning algorithms models

Input parameters			
Parameter	Unit	Minimum	Maximum
$\dot{m}_2$	[kgs^{-1}]	5.5	15.5
U	[Wm^{-2}°C^{-1}]	374.16	604.7
T_R	[°C]	38.6	47.1
T_{Ri}	[°C]	32.2	38.2
T_{Ro}	[°C]	38.2	48.1
Re_2	[–]	2585	7285
Nu_2	[–]	17.6	40.3
h_2	[Wm^{-2}°C^{-1}]	915.9	2098.1
Output parameter			
h_{bd}	[Wm^{-2}°C^{-1}]	374.16	604.7

Decision tree

Decision trees (DT) used in data modelling are widely used in predictive model creation and classification. The DT algorithm uses decision mechanisms based on feature variables arranged in a tree-like structure for prediction and classification. [30]. The DT algorithm uses the M5P algorithm, an extended version of the M5 algorithm [31]. One of the main advantages of model trees is that they can efficiently process large datasets with multiple dimensions. The basic structure consists of three essential parts called a node, branch, and leaf [32]. Construction of the tree uses standard deviation reduction (SDR), which maximizes the expected error reduction at the node, and the SDR is expressed [33]:

$$SDR = sd(S) - \sum_i \frac{S_i}{|S|} \times sd(S) \tag{23}$$

where S is the set of data records reaching the node, S_i is the clusters resulting from the node splitting according to a particular attribute, and sd is the standard deviation [29].

Pace regression

Regression analysis is a widely used data analysis method in statistical analysis, and this method is a technique with both descriptive and predictive purposes [34].

The PACE (Projection Adjustment by Contribution Estimation) regression algorithm is a new approach to fit linear models based on consideration of similar models [35]. Regression analysis is generally used to derive a linear model from a data set. It uses the predictive properties of ordinary little squares for the resulting model. The ordinary little squares method has a solid theory but lacks satisfactory accuracy. The pace regression improves classical ordinary least squares regression by using cluster analysis to evaluate the impact of each variable, estimate their contribution overall regressions, and develop the statistical basis [36].

Wang and Witten [37] developed pace regression and showed that it performs best for high dimensional data than other regression models. Six different regression procedures, named PACE1 to PACE6, were developed, which share a common basic idea that estimated the distribution of the effects of variables from the data and used this to improve modelling. The first four procedures used ordinary least square (OLS) subset selection, including the OLS it self. The PACE 5, on the other hand, was based on the empirical Bayes (EB) method [36]. As with other forms of linear regression, the PR, OLS, and EB methods used to model any parameter is a linear combination of features in format [36]:

$$\text{Modeled parameter} = \alpha_1 A_i + \alpha_2 B_i + \alpha_3 C_i + \alpha_4 D_i + \alpha_5 E_i + ... \tag{24}$$

In eq. (18), expressions such as A, B, C, D, and E were the input parameters in the mesh created for the modeled parameter. The α_i values were the weight coefficients that affect the parameters obtained by the pace regression methods. It was important to note that the resulting model was a linear combination of features. In this way, a simplified forecasting model could be obtained, and the calculation time could be reduced.

Error analysis

Root mean square error (RMSE) analysis is used to determine the accuracy of the models created by machine learning algorithms. The formula and parameters of the RMSE analysis are given in tab. 4 [38].

Table 4. Error analysis and formula

Error analysis	Formulas	Parameters
RMSE	$\sqrt{\dfrac{(P_1 - A_1)^2 + \cdots + (P_n - A_n)^2}{n}}$	Total estimated value, n
		Predicted value, P
		Actual value, A

Result and discussions

In this study, the effects of a deposit that may occur in the cooling system of the I.T.U. Triga Mark-II nuclear research reactor on the average reactor tank water, T_R, temperature values and the total heat transfer of the cooling system were investigated. The previously measured tank temperature data and cooling system flow values [14] were fitted for this research to produce the reactor tank temperature equation, eq. (1). Then, the reactor's overall heat transfer coefficient equation has been delivered, eq. (14), and the effects of a build-up layer that may occur in the second part of the cooling circuit have been revealed. In addition, mathematical equations expressing the heat transfer coefficient of the first layer that may occur in the system were produced using the pace regression algorithm. The results of the study are presented below under two headings as calculation and machine learning algorithms.

Calculation procedure results

The mass-flow rate value in the second part of the heat exchanger used in the reactor cooling system and the temperature change of the reactor cooled by the heat exchanger with the deposit layer are shown in fig. 5. According to the reactor operating conditions, the reactor tank temperature range was chosen as 40-50 °C [1]. This figure has been added to better show the effect of cooling system mass-flow changes on the operating temperature. The T_R temperature value decreased to 13.25 kg/s flow rate and then increased exponentially. This situation indicates that the $\dot{m}_2$ mass-flow rate should not be more than 13.25 kg/s flow rate.

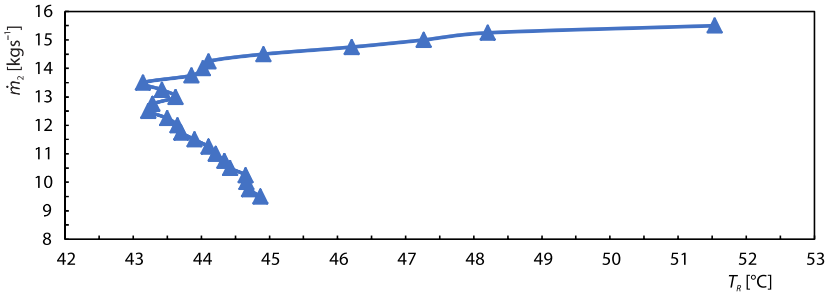

Figure 5. Variation of T_R values according to the mass-flow rate in case of deposit

In fig. 6, the variation of the residual heat transfer coefficient value that may occur in the second part of the heat exchanger according to the $\dot{m}_2$ mass-flow value is shown. The heat transfer value of the deposite layer increased with the decrease of $\dot{m}_2$ flow rate. It can be accepted that the deposit, which is expected to cause poor heat transfer at low flow rates, will also reduce the heat transfer value of the reactor cooling system. Figure 7 shows the change in reactor tank temperature with increasing $\dot{m}_2$ flow rate. This temperature change was investigated according to the presence and absence of deposits in the cooling system heat exchanger. A low T_R temperature value indicates that the reactor cooling system performs cooling with high heat transfer. According to fig. 7, in the case of deposits in the heat exchanger in the cooling system, the reactor temperature increases by an average of 3.5 °C. In addition, the $\dot{m}_2$ value being more than 13.25 kg/s causes the reactor tank temperature to increase.

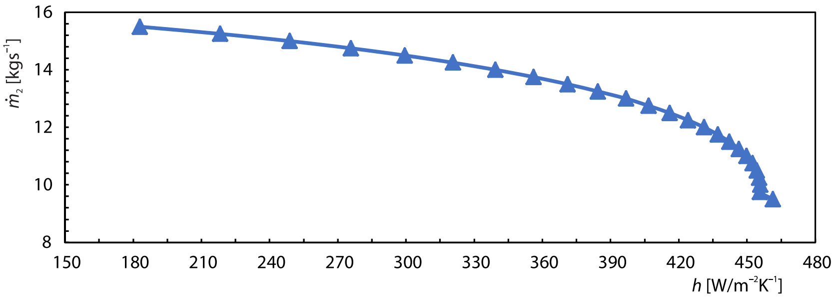

Figure 6. Variation of the heat transfer coefficient of deposit with the mass-flow rate value

Figure 8 presents the variation of the total heat transfer value of the reactor cooling system concerning the deposit in the heat exchanger and the flow rate $\dot{m}_2$. In the absence of deposits, the total heat transfer value of the cooling system increases up to 13.25 kg/s $\dot{m}_2$ flow rate and decreases in subsequent flow values. In the case of deposits in the heat exchanger, the total heat transfer value of the cooling system shows a continuous decrease. According to fig. 8, the average heat transfer coefficient of the cooling system at all flow rates is 311.6 and 572.9 W/m^{2}K, with and without deposits, respectively. The negative effect of the deposit that may form in the heat exchanger on the heat transfer of the reactor cooling system is seen in fig. 8.

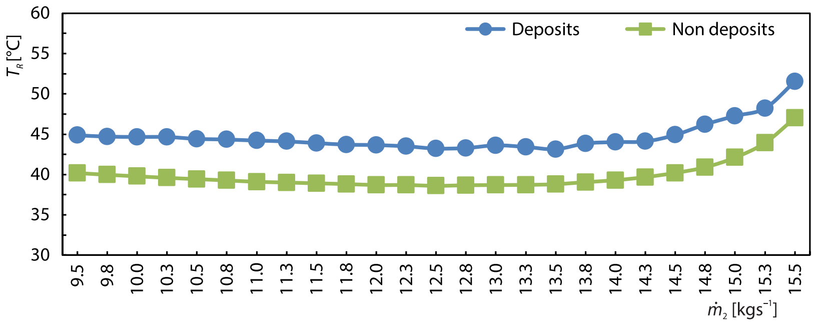

Figure 7. Effect of $\dot{m}_2$ mass-flow rate increase on TR value with and without deposit layer

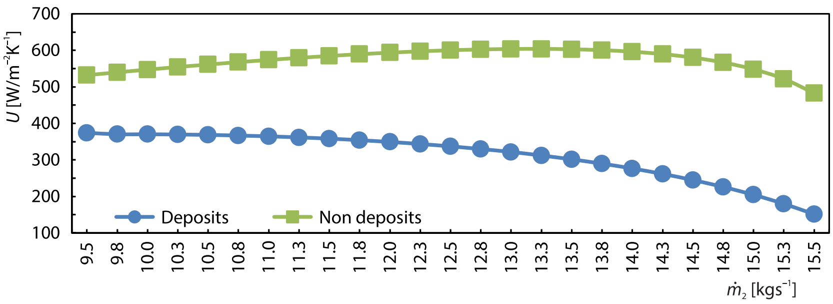

Figure 8. Change of U value with and without deposit layer according to $\dot{m}_2$ value

Machine learning algorithms results

This study used machine learning models to express the effects of deposits in the reactor cooling system on heat transfer. Mathematical equations describing the deposits heat transfer value were obtained using the pace regression algorithm. The M5P decision tree algorithm and pace regression algorithm were used to model the deposits heat transfer value.

In fig. 9, the tree structure created by the M5P decision tree for the h_{bd} values model is seen. Decisions in the tree structure were determined according to $\dot{m}_2$ values, and h_{bd} values were modeled according to the leaf equations of the tree formed as a result of these decisions. These equations are given in tab. 5.

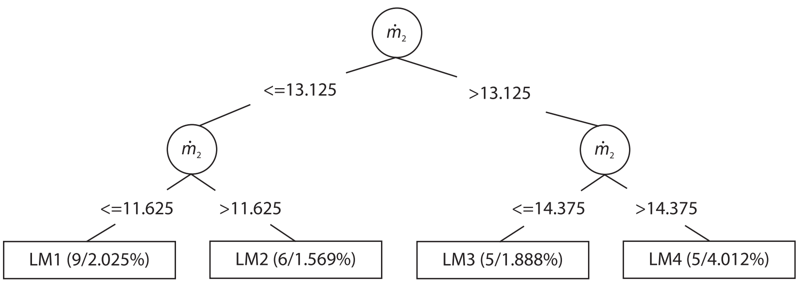

Figure 9. Decision tree structure of the M5P algorithm

Table 6 shows the h_{bd} mathematical equations obtained with OLS and EB in the pace regression algorithm. These equations obtained with the pace regression algorithm were determined according to the total heat transfer coefficient of the reactor cooling system, the cooling system's second circuit heat transfer coefficient, the reactor tank cooling water inlet-outlet temperature, and the reactor tank temperature. These parameters were randomly selected from the input data by the pace regression algorithm.

Table 5. Decision equations in the M5P decision tree

Leaf number (LM)	LM equations
LM num: 1	$h_{bd} = -27.4269\dot{m}_2 + 746.9794$
LM num: 2	$h_{bd} = -31.3061\dot{m}_2 + 791.4761$
LM num: 3	$h_{bd} = -57.5919\dot{m}_2 + 1132.693$
LM num: 4	$h_{bd} = -62.8483\dot{m}_2 + 1208.5806$

Table 6. The deposits heat transfer value equations produced by the pace regression algorithms (OLS and EB)

Pace regression models	Model equations
OLS	$h_{bd} = 2.9U + (-0.3h_2) + 0.5T_{Ri} + 3.7T_{Ro} + 32.2T_R + (-14.4\text{Nu}_2) -1785$
Empirical bayes	$h_{bd} = 2.9U + (-0.6h_2) + 0.5T_{Ri} + 3.7T_{Ro} + 32.2T_R + (-1564)$

Error analysis results of h_{bd} models obtained by machine learning methods are given in tab. 6. All methods modeled the deposits heat transfer value with less than 2% error.

Figure 10 shows the comparison of h_{bd} values calculated with the help of eq. (16) using experimental data and h_{bd} values modeled by machine learning algorithms. In addition, this figure presents the R^2 (correlation coefficient) squared values of the machine learning algorithm models. According to the R^2 value, the least faulty model is the model made with the pace regression algorithm EB method. As shown in fig. 10, the actual and estimated values are pretty close to each other.

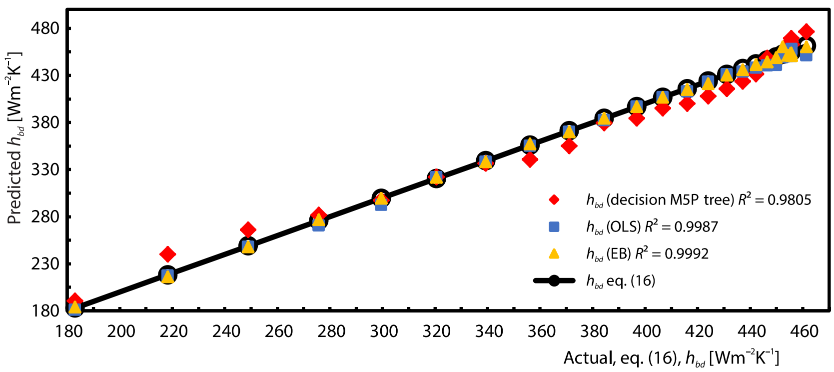

Figure 10. Comparison of experimental h_{bd} data and machine algorithm models h_{bd} data

Conclusion

In the present study, the total heat transfer coefficient of the heat exchanger, which is connected to the first and second sections of the cooling system of the research reactor, was determined. In the second cooling group, the heat transfer coefficient values of a deposit layer covering the pipes and causing an increase in the tank water temperature by worsening the heat transfer were calculated in detail. It has been determined that if the deposit layer covering the outer surface of the pipes in the heat exchanger is cleaned, the average tank water temperature will decrease by approximately 3.5 °C. In addition, modelling was done with pace regression and M5P decision tree algorithms, which are machine learning algorithms, for the deposit layer calculated in the reactor cooling heat exchanger. The deposits heat transfer values obtained with the help of experimental data were modeled by the OLS, EB, and M5P algorithms with RMSE error values of 1.71, 1.66, and 1.99, respectively. A mathematical equation was derived by pace regression for the deposit layer that may occur in the cooling group of the Triga Mark-II nuclear research rector. Thanks to these equations, more detailed information can be obtained about the deposits layer, which is difficult to determine in the reactor cooling group heat exchanger. With the help of the simple but effective mathematical equations derived with pace regression, deposit heat transfer effects can be observed in a heat exchanger simply by knowing the heat transfer and temperature values.

Nomenclature

A_k – slow cross-sectional area, [m^2]
a – weight coefficient
c_p – specific heat capacity, [kJkg^{-1}K^{-1}]
D_{bi} – pipe outer diameter, [m]
D_{bd} – shell diameter, [m]
D_{lm} – average logarithmic diameter, [m]
h_{bd} – deposit layer heat transfer coefficient, [Wm^{-2}K^{-1}]
h_1 – first cooling group heat transfer coefficient, [Wm^{-2}K^{-1}]
h_2 – second cooling group heat transfer coefficient, [Wm^{-2}K^{-1}]
l_s – thermal conductivity of steel, [Wm^{-1}K^{-1}]
l_w – thermal conductivity of water, [Wm^{-1}K^{-1}]
$\dot{m}$ – mass-flow, [kgs^{-1}]
Nu – Nusselt number
P_R – reactor power, [kW]
Pr – Prandtl number
R – heat capacity ratio
Re – Reynolds number
T_{Kg} – cooling tower water inlet temperature, [°C]
T_{Kc} – cooling tower water outlet temperature, [°C]
T_R – average tank water temperature, [°C]
T_{Ri} – tank water inlet temperatures, [°C]
T_{Ro} – tank water outlet temperatures, [°C]
– total heat transfer coefficient, [Wm^{-2}K^{-1}]

Greek symbol

ε – effectiveness of the heat exchanger

References

[1] ***, General Atomic, Triga Mark-II Reactor Mechanical Operation and Maintenance, ITU, Istanbul, Turkey, 1978
[2] Akay, O. E., Constituting the Thermal Model of Triga Mark II Nuclear Research Reactor Cooling System, *Isi Bilim Ve Tek Dergisi*, *Journal Therm. Sci. Technol*., *32* (2012), Jan., pp.109-116
[3] Bouris, D., Bergeles, G., Numerical Calculation of the Effect of Deposit Formation on Heat-Exchanger Efficiency, *Int. J. Heat Mass Transf*., *40* (1997), 17, pp. 4073-4084
[4] Baghdar Hosseini, S., *et al*., Experimental and Numerical Investigation on Particle Deposition in a Compact Heat Exchanger, *Appl. Therm. Eng*., *115* (2017), Mar., pp. 406-417
[5] Guo, Z., *et al*., Mechanisms and Strategies for Ash Deposition Reduction in Flue Gas Heat Exchanger, *Clean Technol Environ Policy*, *24* (2022), June, pp. 77-93
[6] Cassineri, S., *et al.*, Deposition of Corrosion Products under Pressurised Water Nuclear Reactor Conditions: The Effect of Flow Velocity and Dissolved Hydrogen, *Corros Sci*., *159* (2019), 108113
[7] Emani, S., *et al*., Discrete Phase-CFD Simulations of Asphaltenes Particles Deposition from Crude-oil in Shell and Tube Heat Exchangers, *Appl. Therm. Eng*., *149* (2019), Feb., pp. 105-118
[8] Han, Z., *et al.*, Numerical Simulation of Ash Particles Deposition in Rectangular Heat Exchange Channel, *Int. J. Heat Mass Transf*., *136* (2019), June, pp. 767-776
[9] Sun, Q., *et al.*, Study of the Deposition of Graphite Dust in the Inlet Passageway of Intermediate Heat, *Exchanger in VHTR*, *1* (2019), Apr., pp. 29-37
[10] Repić, B. S., *et al*., Investigation of Ash Deposit Formation on Heat Transfer Surface of Boilers Using Coals and Biomass, *Thermal Science*, *23* (2019), Suppl. 5, S1575-S1586
[11] Xu, Z., *et al.*, Simulation of Particle Deposition in a Plate-Fin Heat Exchanger Using a Particle Deposition Model with a Random Function Method, *Powder Technol*., *355* (2019), Oct., pp. 145-156
[12] Levina, T. M., *et al.*, Minimizing Deposit Formation in Industrial Fluid Heat Exchangers, *Proceedings*, IOP Conf. Ser Earth Environ Sci., Vladivastok, Russia, Vol. 666, 2021

[13] Mu, L., *et al.*, Dynamic CFD Modelling Evaluation of Ash Deposition Behavior and Morphology Evolution with Different Tube Arrangements, *Powder Technol*., *379* (2021), Feb., pp. 279-295
[14] Buke, T., *et al*., *An Experience on the Purificiation of Bacterially Infected I. T .U. TRIGA Mark-II Reactor Water*, Mainz, Germany, 1996, pp. 22-25
[15] Akay, O. E., Das, M., Modelling the Total Heat Transfer Coefficient of a Nuclear Research Reactor Cooling System by Different Methods, *Case Stud. Therm. Eng*., *25* (2021), 100914
[16] Durmayaz, A., *et al*., Xenon-Poisoning Method for the Determination of the Average Thermal Neutron Flux, Macroscopic Fission and Total Absorption Cross-Sections, *Kerntechnik*, *62* (1997), 5-6, pp. 245-248
[17] Akay, O. E., Das, M., Modelling the Total Heat Transfer Coefficient of a Nuclear Research Reactor Cooling System by Different Methods, *Case Stud. Therm. Eng*., *25* (2021), 100914
[18] Aboul Khail, A., Erisen, A., Improvement of Plate Heat Exchanger Performance Using a New Plate Geometry, *Arab. J. Sci. Eng*., *46* (2021), Jan., pp. 2877-2889
[19] Wang, X., *et al.*, A Theoretical and Experimental Study of a TBAB Salt Hydrate Based Cold Thermal Energy Storage in an Air Conditioning System, *Therm. Sci. Eng. Prog*., *13* (2019), 100397
[20] Hosseinizadeh, S. E., *et al.*, Energy and Exergy Analysis of Ferrofluid-Flow in a Triple Tube Heat Exchanger under the Influence of an External Magnetic Field, *Therm. Sci. Eng. Prog*., *25* (2021), 101019
[21] Kaya, A., The Effect of Conjugate Heat Transfer on MHD Mixed Convection about a Vertical Slender Hollow Cylinder, *Commun. Non-linear Sci. Numer Simul*., *16* (2011), 4, pp. 1905-1916
[22] Hamzah, J. A., Nima, M. A., Experimental Study of Heat Transfer Enhancement in Double-Pipe Heat Exchanger Integrated with Metal Foam Fins, *Arab, J, Sci, Eng*., *45* (2020), Jan., pp. 5153-5167
[23] Baqir, A. S., *et al.*, Optimisation and Evaluation of NTU and Effectiveness of a Helical Coil Tube Heat Exchanger with Air Injection, *Therm. Sci. Eng. Prog*., *14* (2019), 100420
[24] Cerci, K. N., Das, M., Modelling of Heat Transfer Coefficient in Colar Greenhouse Type Drying Systems, *Sustain*, *11* (2019), 18, 5127
[25] Elhag, A. A., *et al.*, Under Applying Machine Learning and Statistical Models, *Thermal Science*, 24 (2020), Suppl. 1, S131-S137
[26] Alic, E., *et al.*, Heat Flux Estimation at Pool Boiling Processes with Computational Intelligence Methods, *Processes*, *7* (2019), 5, 293
[27] Cerci, K. N., Hurdogan, E., Comparative Study of Multiple Linear Regression (MLR) and Artificial Neural Network (ANN) Techniques to Model a Solid Desiccant Wheel, *Int. Commun. Heat Mass Transf*., *116* (2020), July, 104713
[28] Das, M., *et al*., Detailed Analysis of Mass Transfer in Solar Food Dryer with Different Methods, *Int. Commun. Heat Mass Transf*., *128* (2021), 105600
[29] Wang, Y., Witten, I. H., Induction of Model Trees for Predicting Continuous Classes, *Proceedings*, 9th Eur. Conf. Mach Learn Poster Pap., Hamilton, New Zealand, 1997, pp. 128-137
[30] Li, D., *et al*., Aero-Engine Exhaust Gas Temperature Prediction Based on Lightgbm Optimized by Improved Bat Algorithm, *Thermal Science*, *25* (2021), 2A, pp. 845-858
[31] Quinlan, J. R., Learning with Continuous Classes, *Aust. Jt. Conf. Artif. Intell.*, *92* (1992), Nov., pp. 343-348
[32] Alic, E., *et al*., Heat Flux Estimation at Pool Boiling Processes with Computational Intelligence Methods, *Processes*, *7* (2019), 5, pp. 1-16
[33] Behnood, A., *et al*., Prediction of the Compressive Strength of Normal and High-Performance Concretes Using M5P Model Tree Algorithm, *Constr. Build. Mater*., *142* (2017), July, pp. 199-207
[34] Jiamin, D. L., Shuhong, L. X., Modelling and Optimization of a Chilled-Water Cooling System with Multiple Chillers, *Thermal Science*, *25* (2021), 5B, pp. 3873-3888
[35] Wang, Y., Witten, I. H., Modelling for Optimal Probability Prediction, *Proceedings*, 9th Int. Conf. Mach Learn, Sydney, Australia, 2002, pp. 650-657
[36] Meshkin, A., *et al*., Predicion of Relative Solvent Accessibility Using, *EXCLI Journal*, (2009), 8, pp. 211-217
[37] Wang, J. Y., *et al*., Look-up Tables for Protein Solvent Accessibility Prediction and Nearest Neighbor Effect Analysis, *Biopolymers*, *75* (2004), 3, pp. 209-216
[38] Das, M., Akpinar, E. K., Investigation of Pear Drying Performance by Different Methods and Regression of Convective Heat Transfer Coefficient with Support Vector Machine, *Appl. Sci*., *8* (2018), 2, 215

Paper submitted: January 16, 2022
Paper revised: March 13, 2022
Paper accepted: March 13, 2022